If one assumes a Stokes' effective sphere of radius a to describe ζ, *i.e.*, $\zeta = 6\pi a\eta_s$, then

$$h^* = 0.976a/b \quad (2)$$

If one wants to visualize the bead–spring model with beads of radius a and springs of length b, the ratio a/b has to be smaller than 0.5 to avoid interpenetration of neighboring beads. The values of h^* in Table I are all consistent with this requirement, so the Zimm theory as evaluated by Lodge and Wu leads to values of h^* that intuitively seem reasonable in terms of this crude model.

Since h^* varies so systematically with $[\eta]$, it seems possible to describe h^* as a function of $[\eta]$. In the last column of Table I is given the product $\alpha_\eta h^*$, where α_η is the linear expansion factor of the excluded volume effect as evaluated from the intrinsic viscosity; $\alpha_\eta^3 = [\eta]/[\eta]_\Theta$. The product $\alpha_\eta h^*$ is essentially constant for all combinations of polymer and solvent, except polystyrene in dioctyl phthalate and poly(α-methylstyrene) in α-chloronaphthalene, for which there are reasons for divergence as described above

$$\alpha_\eta h^* = 0.21 \pm 0.02 \quad (3)$$

This result supports the statement that the solvent power is the most important factor determining differences in the hydrodynamic interaction parameter. It is convenient because the dynamic-mechanical properties of usual synthetic polymers at infinite dilution may be predicted if the molecular weight and the intrinsic viscosities for a given solvent and for a Θ solvent are known. Equation 3 together with 1 imply that the hydrodynamic interaction parameter for a good solvent system may be obtained by assuming a uniform expansion of segment lengths by the same factor as is observed for the expansion of overall chain dimensions due to the excluded volume effect. This assumption is sufficient to explain the variation of h^* necessary to describe the dynamic-mechanical properties or the spectrum of relaxation times for the solutions described herein. The assumption may not be consistent with recent theoretical considerations[13] of the dependence of the intrinsic viscosity on solvent, but calculation over a wider range of the number of submolecules N is necessary before this dependence can be discussed any further.

Acknowledgment. This work was supported in part by the National Institutes of Health, the Army Research Office (Durham), and the National Science Foundation. The authors are indebted to Professor A. S. Lodge for supplying us with his numerical results prior to their publication.

Molecular Weight Dependence of the Crystallization Kinetics of Linear Polyethylene. I. Experimental Results[1]

E. Ergoz, J. G. Fatou, and L. Mandelkern*

Department of Chemistry and Institute of Molecular Biophysics, The Florida State University, Tallahassee, Florida 32306. *Received October 26, 1971*

ABSTRACT: The results of a dilatometric study of the crystallization kinetics of molecular weight fractions of linear polyethylene are reported. These data encompass the molecular weight range 4×10^3–8×10^6. Although the usual deviations from the Avrami or Göler–Sachs free-growth formulations are observed, these deviations are systematic with molecular weight and become more pronounced as the molecular weight is increased. There is a one to one correlation between the level of crystallinity at which these deviations occur and the final level of crystallinity that can be attained for each molecular weight. These kinetic results in turn explain the very wide range in values that is observed for all properties. To explain the isotherm shape, we note that over the region of experimental adherance the Avrami exponent is an integral number and varies from four to two as the molecular weight increases. The exponent is independent of temperature except for the very highest crystallization temperatures. At the very highest crystallization temperatures, closer adherance to theory is found, with the implication that if the experiments could be conducted at still higher temperatures the Avrami-type theory would be obeyed. At a fixed temperature the crystallization rate goes through a maximum as a function of molecular weight and the location of the maximum is dependent on the undercooling. Although the very marked negative temperature coefficient gives strong support to nucleation control, it is demonstrated that the rudimentary nucleation theories that have been proposed are not obeyed.

Virtually all thermodynamic, spectral, mechanical and physical properties of linear polyethylene are dependent on molecular weight and on the crystallization conditions.[2–7] A wide range in the values of any specific property is observed for the same chemically constituted polymer. For example, when molecular weight fractions are utilized, the density of melt-crystallized linear polyethylene varies from about 0.99 to 0.92 depending on the molecular weight and the crystallization temperature.[2,8] Based on equilibrium considerations alone, there is no obvious basis for such a range in properties to be observed. Consequently, one is led to seek a kinetic origin for this phenomenon. Since the crystallization of long-chain molecules is by necessity invariably conducted at comparatively large undercoolings, relative to monomeric systems, nonequilibrium properties can easily be expected.

To better understand the factors which govern the properties, therefore, a quantitative molecular understanding of the

(1) This work was supported by a grant from the Army Research Office (Durham).

(2) J. G. Fatou and L. Mandelkern, *J. Phys. Chem.*, **69**, 71 (1965).

(3) L. Mandelkern, A. L. Allou, Jr., and M. Gopalan, *ibid.*, **72**, 309 (1968).

(4) T. Okada and L. Mandelkern, *J. Polym. Sci., Part A-2*, **5**, 239 (1967).

(5) L. Mandelkern, J. M. Price, M. Gopalan, and J. G. Fatou, *ibid., Part A-2*, **4**, 385 (1966).

(6) F. C. Stehling and L. Mandelkern, *Macromolecules*, **3**, 242 (1970).

(7) (a) L. Mandelkern, *Polym. Eng. Sci.*, **7**, (1967); (b) L. H. Tung and S. Buckser, *J. Phys. Chem.*, **62**, 1530 (1958); (c) H. Hendus and K. H. Illers, *Kunstoffe*, **57**, 193 (1967).

(8) E. Ergoz, Ph.D. Dissertation, Florida State University, Dec 1970.

TABLE I
SAMPLE DESIGNATION AND MOLECULAR WEIGHTS

Sample Designation	$\bar{M}_\eta$
RK-5	4,200
RK-7	5,800
RK-9	7,800
RK-12	11,500
RK-14	14,500
R-2-10[a]	20,000
R-2-11[a]	47,000
RS-19	76,000
K-1-16	122,000
RS-20	175,000
R-3-8[a]	200,000
RK-24	284,000
RS-22	660,000
HFD3	1.2×10^6
HFD2	3×10^6
HFB2	5×10^6
HFD1	8×10^6

[a] From ref 2.

crystallization mechanisms and their dependence on molecular weight needs to be developed. Part of the necessary information for this development can be obtained from a study of the crystallization kinetics from the pure melt. Consequently, in this paper we report the results of a study of the overall crystallization kinetics of molecular weight fractions of linear polyethylene. Molecular weights encompassing the range 4.2×10^3–8×10^6 were employed in this work. Our first objective, as is embodied in this report, is to establish the basic experimental facts in as unified a manner as is possible. It is hoped and anticipated that these results will furnish the necessary information and set the basis for a more quantitative understanding of the crystallization process beyond a formal phenomenological analysis.[9]

Experimental Section

Materials. The linear polyethylene fractions used in this work were obtained from unfractionated Marlex-50 (a linear unfractionated polyethylene sample manufactured by Phillips Petroleum Co.) and from Hi-Fax (a linear, high density polyethylene sample, manufactured by Hercules Powder Co. with a reported intrinsic viscosity of 28 and viscosity-average molecular weight of 7×10^6) by either column fractionation or liquid–liquid phase separation methods, respectively. The column fractionation technique used here has been described previously.[2] The highest molecular weight fractions were obtained from the Hi-Fax sample by a liquid–liquid separation method which has been described in the literature.[10-12] The solvent–nonsolvent system used was tetralin and a low molecular weight polyethylene glycol. *N*-Phenyl-2-naphthylamine was added to the solvent to prevent oxidation. The fractionation temperature was 130.0°, and through the entire fractionation process, the system was kept under N_2 atmosphere and exposure of hot solution to air was avoided as much as possible. The fractions that were obtained were precipitated with reagent grade acetone which has been cooled by addition of small pieces of Dry Ice. The sample, which precipitated in the form of a gummy mass, was filtered through sintered glass of medium porosity, washed repeatedly with acetone, and dried in a vacuum oven for 24 hr at 40°. The polyethylene fractions obtained from Hi-Fax are designated by the initials HF in Table I and in the text.

Viscosity Measurements. The determination of the intrinsic viscosities of the fractions obtained from column fractionation has been described previously.[2] The intrinsic viscosities of the very high molecular weight fractions, obtained by the liquid–liquid phase separation method, were determined in an Ubbelohde-type four-bulb shear dilution viscometer. Flow-time measurements were obtained while the solutions were in a nitrogen atmosphere by using a viscometer head designed for this purpose.[13] For these high molecular weight samples, the specific viscosity, at a fixed concentration, was plotted against the shear rate. For sufficiently dilute solutions, the data could be extrapolated linearly to zero shear rate. The intrinsic viscosity of each fraction was determined in the conventional manner by extrapolating the linear plot of (η_{sp}/c) against concentration (c) to zero concentration. Viscosity-average molecular weights were obtained from the relation

$$[\eta] = (6.20 \times 10^{-4})M_\eta^{0.7} \quad (1)$$

given by Chiang[14] for decalin at 135.0°. The viscosity-average molecular weights for the polyethylene fractions studied in this work are given in Table I. For samples whose molecular weights were less than 1×10^6, the ratio of the weight- to number-average molecular weight was in the range 1.1–1.2.

Crystallization Kinetics. The crystallization kinetics studies were carried out using dilatometric techniques previously described in detail.[15-17] The samples were molded in a Carver hot press under a nitrogen atmosphere into approximately 0.5–1-mm thick, bubble-free films. Infrared spectra were obtained for each sample in order to check the possibility of any oxidation occurring during the preparative procedure. Those films showng an ir peak around the 1725-cm^{-1} region were not used. Because of the small amount of sample available, a slight modification was made in the dilatometer described by Baker and Mandelkern.[17] This modification consisted of using a spacer whose diameter was about 1 mm less than that of the dilatometer bulb. About 100 mg of bubble-free polymer film was accommodated in a small saddle in the spacer. The ends of the spaces were sealed around the ends of the bulb. The stem of the dilatometer was 12–15 cm long and consisted of a 1-mm diameter precision bore tubing graduated in millimeters along its length. After sealing, the dilatometer bulb containing the sample was evacuated overnight and filled with triply distilled mercury under vacuum. The amount of mercury in each dilatometer varied from 1.5 to 2 cm^3. The freshly prepared dilatometer was placed in a silicone oil bath at room temperature and the bath temperature was slowly raised to 160°. The dilatometer was kept at this temperature for 80 min. This procedure ensured the complete melting of the sample. The dilatometer was then quickly transferred to another silicone oil bath set at a predetermined crystallization temperature and controlled to better than 0.01°. Temperature control was provided by a modified thyraton relay of the type described by Sturtevant,[18] which assured constant operation of the bath over the long periods of time necessary for these studies.

The mercury level in the dilatometer capillary started to fall with the transfer from the melting bath to the crystallization bath. This decrease was very rapid for the first 30 sec after the transfer. About 1.5 min after the transfer, however, the mercury height remained constant until crystallization ensued. The time of transfer was taken as zero time and the level of the mercury column was recorded as a function of time. The observed mercury column height at a given time was utilized to calculate the specific volume $\bar{v}_t$ of the partially crystalline sample. This quantity, in turn, was used to calculate the degree of crystallinity, $1 - \lambda$, at that time, assuming the additivity of specific volumes.[19]

(9) L. Mandelkern, "Crystallization of Polymers," McGraw-Hill, New York, N. Y., 1964.
(10) N. Nasini and C. I. V. Mussa, *Macromol. Chem.*, **22**, 59 (1957).
(11) H. Okamoto and K. Sekikawa, *J. Polym. Sci.*, **55**, 597 (1961).
(12) H. Okamota, *ibid.*, *Part A*, **2**, 3451 (1964).
(13) P. F. Onyon in "Techniques of Polymer Characterization," P. W. Allen Ed., Butterworths, London, 1961.
(14) R. Chiang, *J. Polym. Sci.*, **36**, 91 (1959).
(15) P. J. Flory, L. Mandelkern, and H. K. Hall, *J. Amer. Chem. Soc.*, **73**, 2352 (1951).
(16) L. Mandelkern and P. J. Flory, *ibid.*, **73**, 3206 (1951).
(17) C. H. Baker and L. Mandelkern, *Polymer*, **7**, 7 (1966).
(18) J. M. Sturtevant in "Physical Methods in Organic Chemistry," Vol. 1, A. Weissberger, Ed., Interscience, New York, N. Y., 1945, p 327.
(19) R. Chiang and P. J. Flory, *J. Amer. Chem. Soc.*, **83**, 2057 (1961).

The densities of the crystalline samples were determined at 25° in a toluene–dioxane density-gradient column utilizing methods previously described in detail.[2,20]

Morphology. The morphological features of the melt-crystallized samples were investigated by electron microscopy utilizing the selective-oxidation technique developed by Palmer and Cobbold.[21,22] Approximately 0.5 × 0.5 cm strips of polyethylene films, either well crystallized at 130° or quenched in liquid nitrogen, were digested in 90% reagent grade fuming nitric acid at 80° for a period of time ranging from 48 to 200 hr. During the process, the polymer strips were kept immersed in the acid with the aid of glass plugs. Each tube, together with the acid and polymer strip, was immersed in a large beaker containing distilled water and the acid washed out by changing the water repeatedly. After a 24-hr washing period, the polymer strips, which retained their original shapes, were taken out of water and stored in ethyl alcohol for 24 hr. The oxidized polymer samples, which had become very brittle, were mechanically crushed in ethyl alcohol, and a small droplet of this suspension was placed on a 200-mesh electron microscope grid. The grids thus prepared were dried overnight in a vacuum oven at room temperature. Electron micrographs were taken with a Phillips 200 electron microscope.

Results and Discussion

General Results. Depending on the molecular weight, quantitative kinetic data could be obtained in the temperature interval from 125 to 132°. At lower temperatures, the crystallization rates become so rapid as to preclude accurate measurements by the dilatometric technique. On the other hand, at higher temperatures the rates become too slow to allow for the collection of a sufficient amount of data in a reasonable time period. For example, at 121°, for M = 76,000, it takes about 1 min for half of the crystallization to occur. However, we estimate from the present results that for this molecular weight at 133° it would take about 4×10^5 min (*ca.* three-quarters of a year) to achieve the same extent of transformation. The total crystallization times involved in the results reported here range from about 100 min at the lowest crystallization temperature to about 6 weeks at the highest one. The accessible temperature range is, however, very dependent on molecular weight. For molecular weights greater than 1×10^6, the kinetics could be studied in the range 125–130°. For the lowest molecular weight samples, the highest crystallization temperature that could be practically studied was 128°. The utilization of molecular weight fractions has enabled us to study the transformation kinetics at temperatures as high as 132° for M = 76,000–660,000. These represent the highest crystallization temperature reported heretofore for linear polyethylene. The consequences of these high-temperature measurements and their utility in helping to elucidate the crystallization process will be discussed subsequently.

Before presenting and analyzing the actual kinetic data, it is important to assess whether there is any influence of the melting conditions on the subsequent crystallization behavior. The important variables of concern are the initial temperature of the melt and the time at which the sample is held at this temperature. To examine this problem, the following experiments were performed using fractions of M = 14,000, 285,000, and 660,000, respectively. Before each crystallization, the dilatometer was kept in the melting bath for periods of time which varied from 10 to 80 min at a series of predetermined temperatures in the range of 139–180°. The

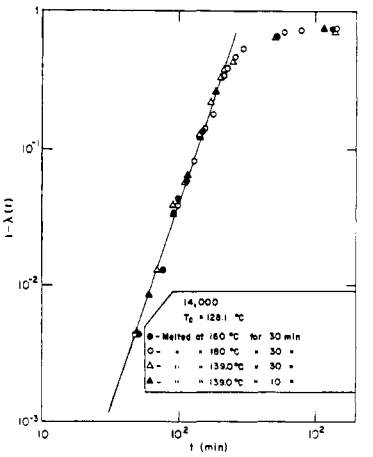

Figure 1. Plot of degree of crystallinity $1 - \lambda$ as function of log t for fraction M_η = 14,000 for different conditions of melt as is indicated.

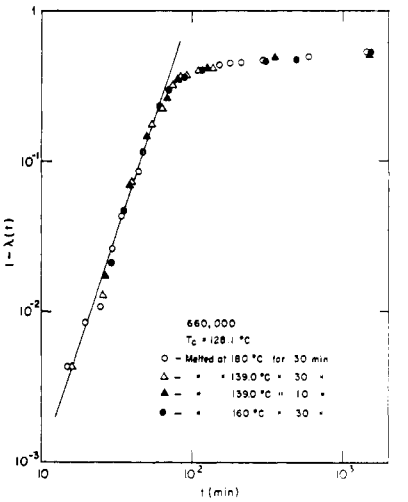

Figure 2. Plot of degree of crystallinity $1 - \lambda$ as function of log t for fraction M_η = 660,000 for different conditions of melt as is indicated.

results of these experiments are summarized in Figures 1 and 2 as plots of the degree of crystallinity against log time. As is readily discerned from these figures, for each fraction in this molecular weight range, the crystallization isotherms are quantitatively independent of the precrystallization treatment in the molten state. We should note that the lowest temperature at which the samples were held is only about 1.5° higher than the directly observed melting temperature. Thus, as long as the sample is rendered completely molten, the temperature of the melt and time held there have no influence on the ensuing crystallization isotherm. These observations are in agreement with previous studies of unfractionated polyethylene[9] and the more recent work of Vidotto and Kovacs[23] and Banks, *et al.*[24] Based on these results we have, in this molecular weight range, adopted the procedure of maintaining the sample at 160° for 80 min prior to transfer to the crystallization bath.

However, for molecular weights equal to or greater than 1.2×10^6, the reproducibility of the isotherms and inde-

(20) R. K. Sharma and L. Mandelkern, *Macromolecules*, **2**, 266 (1969).
(21) R. P. Palmer and A. J. Cobbold, *Macromol. Chem.*, **74**, 174 (1964).
(22) A. Keller and S. Sawada, *ibid.*, **74**, 190 (1964).
(23) G. Vidotto, D. Levy, and A. J. Kovacs, *Kolloid-Z. Z. Polym.*, **230**, 19 (1969).
(24) W. Banks, M. Gordon, R. J. Roe, and A. Sharples, *Polymer*, **4**, 61 (1963).

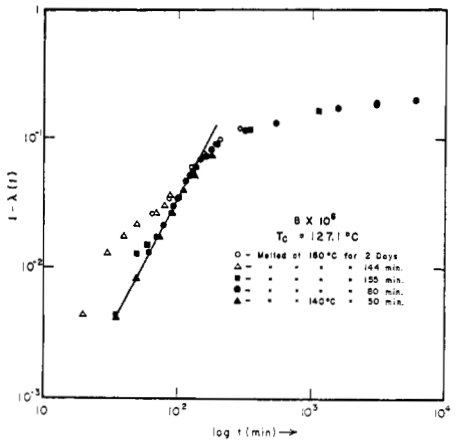

Figure 3. Plot of degree of crystallinity $1 - \lambda$ as function of log t for fraction $M_\eta = 8 \times 10^6$. The different conditions of the melt are indicated in sequential order.

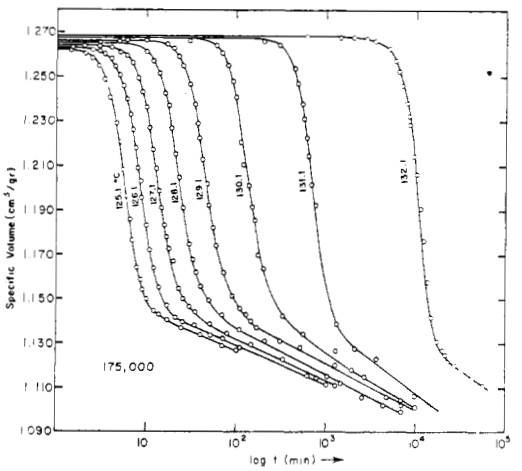

Figure 4. Plot of specific volume against log t at indicated temperatures for fraction $M_\eta = 175{,}000$.

pendence of prior thermal history in the melt were not as easily attained. As is indicated in Figure 3, for a molecular weight of 8×10^6, the isotherm obtained after the initial melting at 160° was unusual in the sense that it did not fit into any particular pattern with respect to the results for the lower molecular weights. However, if the sample was never cooled below the crystallization temperature, then on the third and subsequent melting and crystallization the results, although different from the initial crystallization, were reproducible with one another. As is indicated in the figure, the same results were now obtained irrespective of whether the melting temperature was 140 or 180°. As will be seen below, these results now followed the pattern established by the lower molecular weights in the series. It would appear that because of the initially high levels of crystallinity and very high viscosity of the melt, the first melting treatment did not yield a completely random molten system.

A typical specific volume–time plot is given in Figure 4. The general characteristics of the crystallization kinetic isotherms, for all molecular weights, are qualitatively very similar to those that have been reported for a large number of unfractionated polymeric systems.[9] There is in all cases an initial time period where crystallinity is not detected. This is followed by an accelerated rate of development of transformed material. Finally there is a leveling off in the

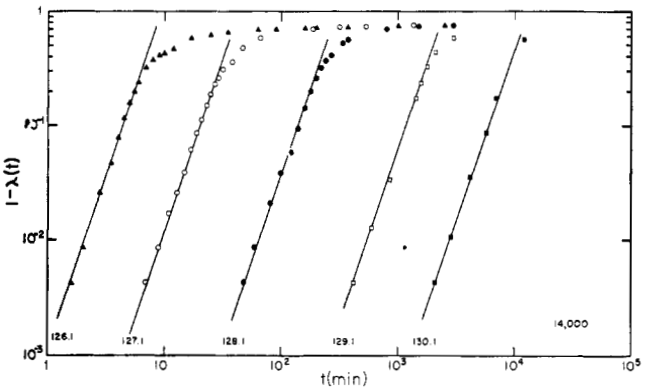

Figure 5. Double logarithmic plot of $1 - \lambda$ against t at indicated temperatures for $M_\eta = 14{,}000$.

crystallization rate as a pseudoequilibrium degree of crystallinity is approached. In a very general sense, there would not appear to be much difference between these data and those for unfractionated systems. However, the strong influence of molecular weight on the isotherm shape, time scale, and temperature coefficient will be seen in the more detailed analysis of the data that is given below. It is important to note at this point that the crystallization process, as evidenced by the directly measured specific volume, is a continuous one. Although there are clearly several regions in the isotherms where the rates of change of crystallinity with time are very different from one another, no discontinuities of the type discussed by Rybhikar[25,26] for poly(ethylene terephthalate), polycaproamide, polychlorotrifluoroethylene, and branched polyethylene; by Sharples and Swinton[27] for poly(decamethylene terephthalate); and by Matsuoka[28] for polyethylene are observed.

Free-Growth Analysis. In order to present and analyze these data in more detail, it is convenient to utilize the Göler–Sachs so-called "free-growth" approximation as background or frame of reference.[29] The essence of this concept is summarized in the integral equation given by

$$1 - \lambda(t) = (\rho_c/\rho_l) \int_0^t v(t, \tau) N(\tau) \lambda(\tau) d\tau \qquad (2)$$

Here ρ_c and ρ_l are the densities of the pure crystal and liquid, respectively; $v(t, \tau)$ is the volume at time t of a growing center formed at time $\tau < t$; and $N(\tau)$ is the nucleation frequency per unit volume of untransformed material per unit time. Before one can proceed to solve eq 2, the form of $N(\tau)$ and $v(t, \tau)$ needs to be specified. We assume, solely for the purpose of developing an equation for data presentation, a steady-state nucleation rate and a lineal rate of growth of a transformed center after it is formed. Thus $N(\tau)$ is assumed constant and $v(t, \tau)$ can be expressed as

$$v(t, \tau) = f_i G^i (t - \tau)^i \qquad (3)$$

Here G is the rate of growth and the exponent i defines the geometry of the growth, *i.e.*, one, two, or three dimensional. The constant f_i is a shape factor. The solution of eq 2 for $i = 3$ has been given by Göler–Sachs as[29]

$$1 - \lambda(t) = 1 - \cosh k_3 t \cos k_3 t \qquad (4)$$

(25) F. Rybhikar, *J. Polym. Sci.*, **44**, 517 (1960).
(26) F. Rybhikar, *ibid.*, **61**, 2031 (1963).
(27) A. Sharples and F. L. Swinton, *Polymer*, **4**, 119 (1963).
(28) S. Matsuoka, *J. Polym. Sci.*, **42**, 511 (1960).
(29) V. Göler, F. Sachs, and G. Sachs, *Z. Phys.*, **77**, 281 (1932).

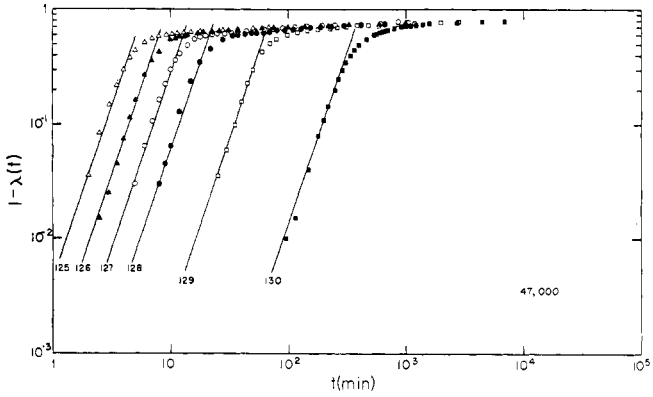

Figure 6. Double logarithmic plot of $1 - \lambda$ against t at indicated temperatures for $M_\eta = 47{,}000$.

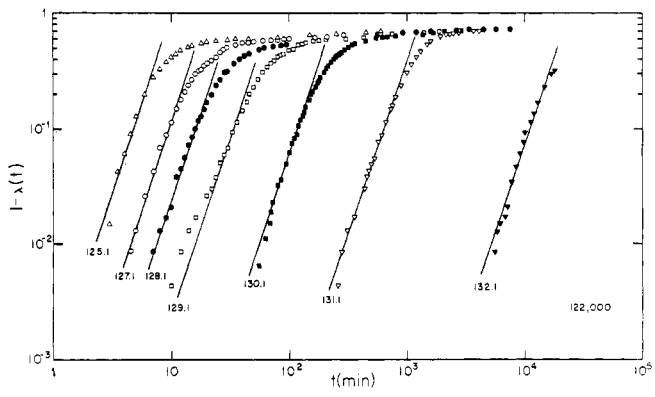

Figure 7. Double logarithmic plot of $1 - \lambda$ against t at indicated temperatures for $M_\eta = 122{,}000$.

For the other two cases, $i = 1$ and $i = 2$, the equation can be solved in a straightforward manner.[8] Unfortunately, as has been pointed out previously, these equations do not provide for a natural termination to the crystallization process, since real solutions exist for $1 - \lambda(t) > 1$. Therefore, its use must be arbitrarily restricted to the physically sensible region $0 \leq 1 - \lambda(t) \leq 1$.

For the initial portions of the transformation, the equations can be series expanded in terms of $k_i t$. When the first two terms of the expansion are retained, it is found that

$$1 - \lambda(t) \cong (k_3 t)^4/4 \tag{5}$$

$$1 - \lambda(t) \cong (k_2 t)^3/6 \tag{6}$$

$$1 - \lambda(t) \cong (k_1 t)^2/2 \tag{7}$$

for the respective growth geometries. These expressions are commonly called the free-growth approximations. They suggest that as the most rudimentary analysis of the kinetic data a double logarithmic plot be made of $1 - \lambda(t)$ against time. Typical experimental results, covering the complete molecular weight range studied, are plotted in Figures 5–9 according to the suggestion of eq 5–7. Despite the obvious simplicity of the analysis, we note from these figures that there is a rather good adherance of the experimental data to this theoretical development. A linear relation is obtained for a significant portion of the total transformation. For the lower molecular weights, deviations do not occur until high levels of crystallinity are developed. However, as the molecular weight increases the discrepancy between this simple theory and experiment occurs at progressively lower levels of crystallinity.

For any given molecular weight fraction, the slopes of the linear portions are found to be independent of temperature. (Four exceptions to this general statement occurred. For molecular weight fractions 7800 and 11,500, the isotherms at 129.1 and 130.1° have slopes equal to 4. At lower crystallization temperatures, the slopes for both these fractions are 3. These are the only exceptions that have been experimentally observed to the generalizations cited above.) Most important, however, is the fact that the slopes of these straight lines have an integral value which depends on molecular weight. For the two lowest molecular weights studied, $M =$ 4200 and 5800, the slope is 4. As the molecular weight increases, up to and including $M = 1.2 \times 10^6$, the slope is 3. For the highest molecular weights, the slope has been reduced to 2. The straight lines in the figures are drawn with slopes which have the indicated exact integral value. The

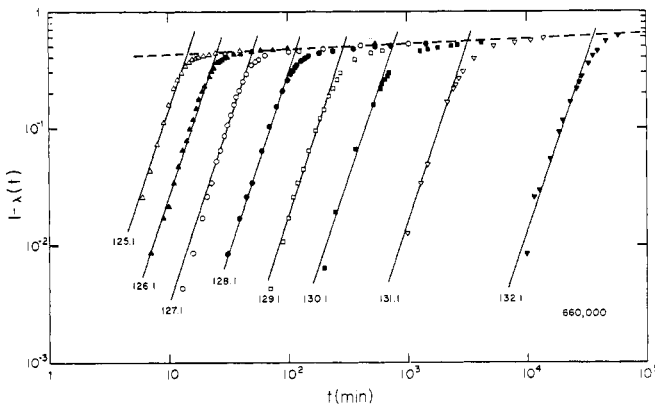

Figure 8. Double logarithmic plot of $1 - \lambda$ against t at indicated temperatures for $M_\eta = 660{,}000$.

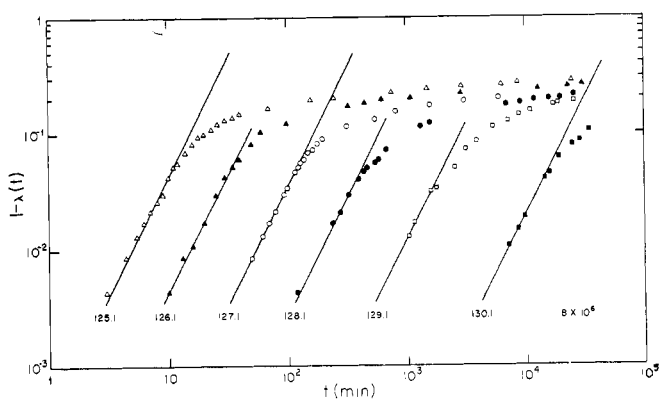

Figure 9. Double logarithmic plot of $1 - \lambda$ against t at indicated temperatures for $M_\eta = 8 \times 10^6$.

extraordinary close adherance of these straight lines to the experimental data is quite clear. Hence, the fact that integral values for the slope are obtained is quite important. The change in this quantity with molecular weight must be an important factor in elucidating the crystallization mechanisms. As will be seen below, the magnitude of the slope corresponds to the exponent n in the Avrami relation.

Another important observation that can be made from these data is specifically illustrated in Figure 8. After the deviations from linearity develop, the experimental results for each temperature, for a given molecular weight, form a common straight line of very small slope. This observation is easily demonstrated for molecular weight fractions less than

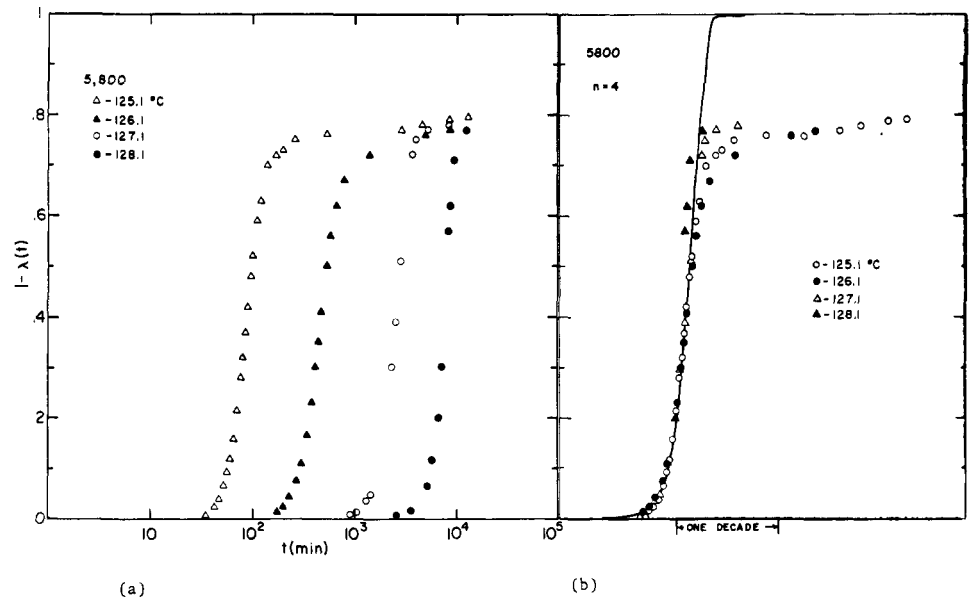

Figure 10. (a) Plot of $1 - \lambda$ against $\log t$ at indicated temperatures for $M = 5800$. (b) Superimposed isotherms. Solid line, theoretical Avrami, $n = 4$.

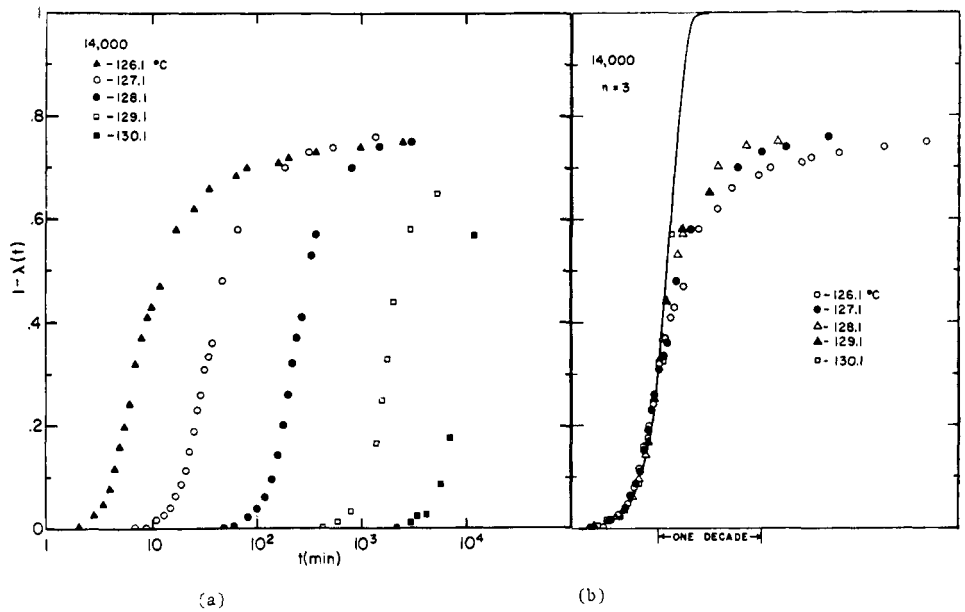

Figure 11. (a) Plot of $1 - \lambda$ against $\log t$ at indicated temperatures for $M = 14{,}000$. (b) Superimposed isotherms. Solid line, theoretical Avrami, $n = 3$.

3×10^6. For higher molecular weights, although the same tendency clearly manifests itself (see Figure 9 for example), the actual formation of a common line cannot be observed because of the very long crystallization times that are involved. The generality of the observation appears to be warranted, however, and indicates that the leveling-off value of the degree of crystallinity, or the pseudoequilibrium value at very long times, is independent of the crystallization temperature.

Avrami Formulation and Superposition. The double-logarithmic plots of Figures 5–9 were convenient in illustrating the adherence to simple theory of a large portion of the transformation. However, this method of presenting the data is very insensitive to the higher levels of crystallinity, where the deviations from the free-growth theory manifest themselves. To properly assess this region we present in Figures 10–15 (left-hand curves) typical data, covering the complete molecular weight range, as linear plots of the degree of crystallinity as a function of $\log t$. The insensitivity to the higher levels of crystallinity of the previous plots has now been removed. In these plots, one observes the autocatalytic nature of the process at the early stages of the crystallization and then a very marked retardation in the rate of the transformation so that the increase of crystallinity with time proceeds very slowly. For a given molecular weight, except for the time scale of the crystallization, all the isotherms have the same general character. However, when the different molecular weights are compared, the extent of the transformation at which the crystallinity rate becomes retarded is very dependent on molecular weight.

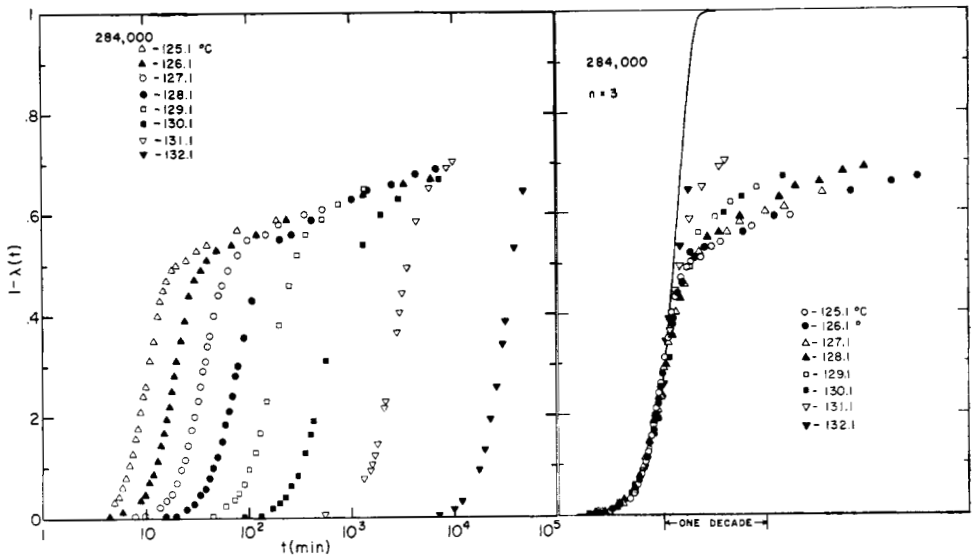

Figure 12. (a) Plot of $1 - \lambda$ against $\log t$ at indicated temperatures for $M = 284{,}000$. (b) Superimposed isotherms. Solid line, theoretical Avrami, $n = 3$.

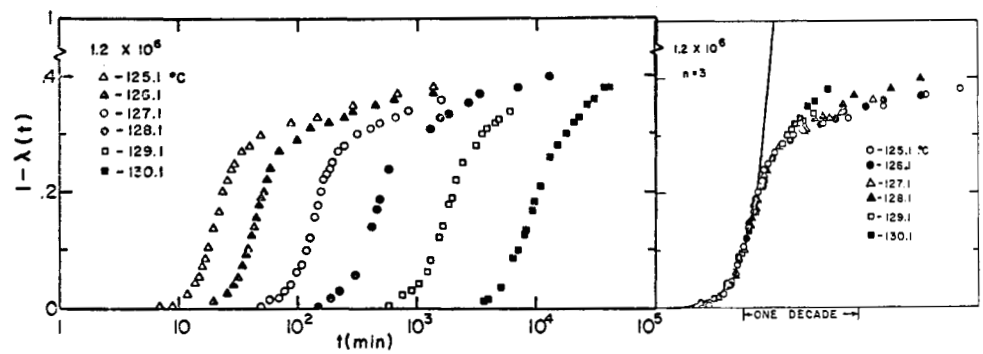

Figure 13. (Left) Plot of $1 - \lambda$ against $\log t$ at indicated temperatures for $M = 1.2 \times 10^6$. (Right) Solid line, theoretical Avrami, $n = 3$.

In Figures 10–15 (right-hand curves) the experimental isotherms, for a given molecular weight fraction, were superposed upon one another by shifting each one along the log time axis until the best composite was obtained. The superposition was performed on the basis of the absolute degree of crystallinity. The solid line that is drawn in each figure represents the theoretical Avrami isotherm which gives the best agreement with the early stages of the transformation.[30] The Avrami equation can be written in general form as[9,30a]

$$1 - \lambda(t) = 1 - \exp(-kt^n) \qquad (8)$$

It differs in concept from the Göler–Sachs treatment in assuming that when two growing centers impinge upon each other growth ceases. Mathematically, eq 8 reduces in form to the Göler–Sachs expression for small extents of transformation. The Avrami exponent n is thus the slope of the double logarithmic plot of $1 - \lambda$ against t.

The agreement of the experimental data with the Avrami formulation is about the same as with the free-growth approximation. A more detailed comparison indicates that deviations from either of the theories occur at about the same level of crystallinity. Thus the introduction of the impingement factor does not contribute in any significant way to a better agreement between theory and experiment for the

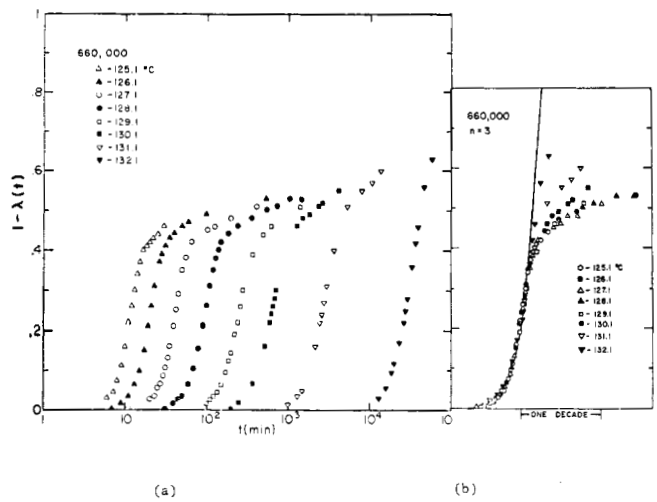

Figure 14. (a) Plot of $1 - \lambda$ against $\log t$ at indicated temperatures for $M = 660{,}000$. (b) Solid line, theoretical Avrami, $n = 3$.

(30) (a) M. Avrami, *J. Chem. Phys.*, **7**, 1103 (1939); *ibid.*, **8**, 217 (1940); *ibid.*, **9**, 177 (1941). (b) Since the ultimate aim of the analysis is to understand the crystallization mechanisms which involve the factors that control the final level of crystallinity that is attained, the data are not normalized.[30a,c] Thus, the analysis is conducted on an absolute basis. (c) L. Mandelkern, F. A. Quinn, and P. J. Flory, *J. Appl. Phys.*, **25**, 830 (1954).

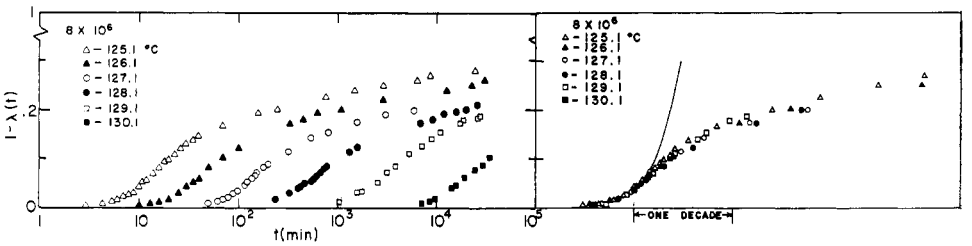

Figure 15. (Left) Plot of $1 - \lambda$ against $\log t$ at indicated temperatures for $M = 8 \times 10^6$. (Right) Solid line, theoretical Avrami, $n = 2$.

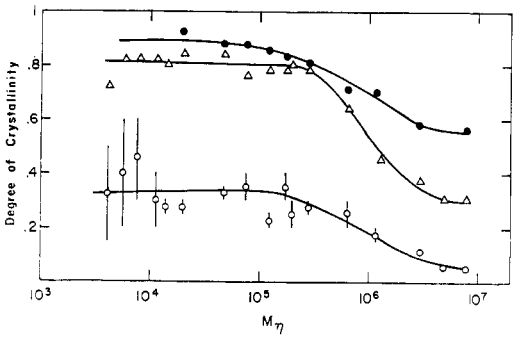

Figure 16. Plot of $1 - \lambda$ against molecular weight: $1 - \lambda$ at deviations from Avrami theory (○), final $1 - \lambda$ at crystallization temperature (△), $1 - \lambda$ after cooling to room temperature (●).

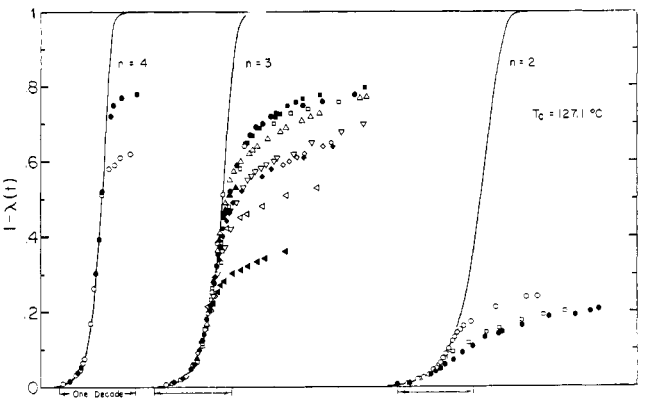

Figure 17. Plot of $1 - \lambda$ against $\log t$ for crystallization at 127.1° for indicated molecular weights: $n = 4$, 4200 (○), 5800 (●); $n = 3$, 7800 (○), 11,500 (●), 14,000 (□), 20,000 (■), 47,000 (△), 76,000 (▲), 122,000 (▽), 175,000 (▼), 200,000 (◊), 284,000 (◆), 660,000 (▷), 1.2×10^6 (◀); $n = 2$, 3×10^6 (○), 5×10^6 (●), 8×10^6 (□). Solid lines, theoretical Avrami with indicated n values.

crystallization of long-chain molecules from the melt. Consequently, our understanding is not advanced any further. We have seen that for the extent of the transformation where there is agreement between experiment and theory, the Avrami exponent is a well-defined integer and is consistent with the physical concepts embodied in the theory.

Figures 10–15 (right-hand curves) also demonstrate the superposability principle rather vividly. For all the molecular weights studied and for crystallization at temperatures of 129.1° and below the isotherms are, with minor exception, superposable over the complete extent of the transformation. This includes not only the autocatalytic region but the final stages of the transformations as well. Thus the same time–temperature reduced variable is maintained throughout the transformation for a given molecular weight. Therefore, the temperature coefficients of the processes involved in the retarded or "tail portion" of the isotherms are the same as for the initial parts of the transformation. However, for crystallization temperatures of 130° and greater, the final portions of the isotherms are no longer superposable with one another and with those obtained at the lower temperature. This point is particularly well illustrated in Figures 12 to 14 (right-hand curves). On the other hand, at these higher temperatures adherence to theory is obtained for much larger levels of crystallinity. This can be most clearly seen in Figure 14b for $M = 660{,}000$. As the crystallization temperatures are increased from 129 to 132°, better adherence to the solid line is found and the final level of crystallinity that is attained is substantially increased. These results for the high crystallization temperature imply that if it were possible, from the point of view of the time involved, to conduct the crystallization at more elevated temperatures, greater levels of crystallinity would be attained and better agreement with simple theory would be observed.

Detailed Influence of Molecular Weight. When the data are examined in more detail, an interesting correlation is found between the level of crystallinity at which deviations from the Avrami theory are observed and the final level of crystallinity which is attained. These findings are summarized in Figure 16. For the lower molecular weights, $\lesssim 1 \times 10^5$, the deviations set in at about a 30% level of crystallinity, while about 80% crystallinity is attained at the crystallization temperature. However, as the molecular weight increases the deviations occur at successively lower levels of crystallinity. For the highest molecular weight fractions, they take place when only a small per cent of the transformation has occurred. Concomitantly, the final level of crystallinity that is reached is also decreasing. A level of about 30% is attained for the highest molecular weights. Thus, the factors which cause the deviation from the simple postulates of the Avrami theory (or the free growth) are the same which control the final level of crystallinity at the crystallization temperature. A variety of detailed studies have shown that the level of crystallinity is the major determinant of thermodynamic, physical and mechanical properties of crystalline polymers in general and linear polyethylene in particular.[3,4,6,7a,8] Upon cooling to room temperature, the change in the level of crystallinity with molecular weight is still maintained, as can be seen from the third curve in Figure 17. Only a small increase in crystallinity is incurred at the lower molecular weights, while a disproportionately higher increase takes place at the higher molecular weights.[2] It would appear, therefore, that the same factors which cause the deviations from the free-growth or Avrami theories determine the properties of crystalline polymers through control of the level of crystallinity. An understanding of these factors would thus lead to an understanding of properties. It becomes clear, therefore, that the large variation in properties which is observed is a consequence of kinetic factors.

The influence of molecular weight on the crystallization process can be seen in more detail in the plots of Figures 17 and 18. Here, for two representative temperatures, the isotherms for the different molecular weights have been superposed on one another. This superposition with molecular weight can, of course, only be accomplished for the extent of the transformation that agrees with theory. The superposed curves naturally divide themselves into three categories based on the three Avrami n values that have been found. Both the agreement with theory and the final level of crystallinity are clearly illustrated. For example, for the very low molecular weight fractions, where $n = 4$, very good agreement with theory is found for levels of crystallinity approaching 80%. As the molecular weight increases up to $M = 1.2 \times 10^6$, the crystallization process starts in exactly the same way and the shapes of the isotherms are indistinguishable from one another and the Avrami or free-growth formulation. As the transformation progresses, the previously noted influence of molecular weight on the deviations from theory and on the final level of crystallinity is clearly discerned. For the very highest molecular weights there is a change in the initial portion of the process to $n = 2$ and much lower levels of crystallinity are attained.

The discussion heretofore has been concerned mainly with the relationship of the isotherm shapes to the Avrami or free-growth theory. Despite major discrepancies from theory, the isotherms are found to be continuous curves with a marked retardation in rate as an apparent final level of crystallinity is approached. The influence of molecular weight on this final or tail portion of the isotherm can be summarized by the fact that for all fractions having a given n value these portions of the isotherms for a given temperature can be superposed by shifting along both the time and degree of crystallinity axes. By this procedure the tail portions of the isotherms of different molecular weights can be brought into exact coincidence with one another. Thus, except for the addition of a constant, the tail portions of the isotherms are independent of molecular weight.

The influence of molecular weight on the time scale of the crystallization process, *i.e.*, on the crystallization rate, is also very pronounced. A summary of the crystallization time scale is given in Figure 19. Here is plotted, on a double logarithmic scale, the time required for 1% of the absolute amount of crystallinity to develop, $\tau_{0.01}$, as a function of molecular weight. Also included in this plot are the recent data, reported by Fatou and coworkers, for the very rapid crystallization below 125° as determined by differential scanning calorimetry.[31] The data obtained by the two different techniques are contiguous with one another. Certain very important features of the crystallization process manifest themselves in this figure, and a preliminary report of some of these results has been given.[32]

In the lower molecular weight range, the crystallization times decrease over several decades as the molecular weight is increased. This increase in the crystallization rate is observed at all the accessible crystallization temperatures. However, a minimum in the time scale (maximum in the crystallization rate) is reached. The molecular weight at which the crystallization rate achieves its maximum value is dependent on the crystallization temperature. For the highest crystallization temperatures the maximum in the rate occurs in the range of $M = 1\text{–}2 \times 10^5$. The locus describing the maximum decreases with decreasing temperature and is in the range $1\text{–}2 \times 10^4$ for the lowest attainable crystallization temperature.

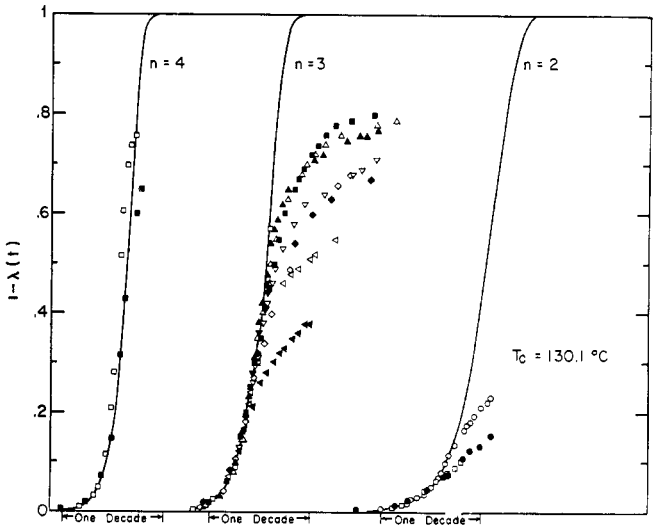

Figure 18. Plot of $1 - \lambda$ against $\log t$ for crystallization at 130.1° for indicated molecular weights: $n = 4$, 7800 (□), 11,500 (■); $n = 3$, 14,000 (□), 20,000 (■), 47,000 (△), 76,000 (▲), 122,000 (▽), 175,000 (▼), 200,000 (◇), 284,000 (◆), 660,000 (◁), 1.2×10^6 (◀); $n = 2$, 3×10^6 (○), 5×10^6 (●), 8×10^6 (□). Solid lines, theoretical Avrami with indicated n values.

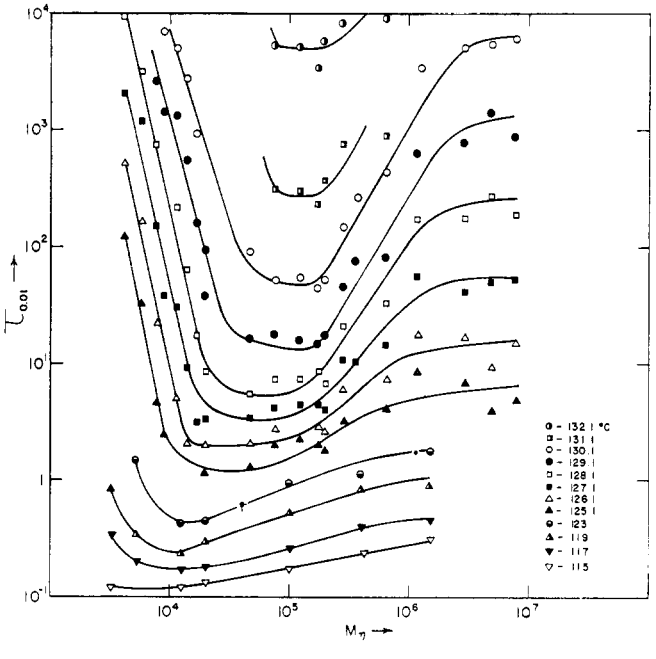

Figure 19. Double logarithmic plot of $\tau_{0.01}$ against molecular weight for indicated crystallization temperatures.

Concomitantly, $\tau_{0.01}$ at the maximum rate decreases from about 10^4 min at 132° to less than 1 min at 123°. At the left-hand side of the maximum, the relation between $\tau_{0.01}$ and M appears, within the experimental error, to be independent of the crystallization temperature. On the other hand, for molecular weights which exceed that for the maximum rate of crystallization, this relation is clearly very dependent on the crystallization temperature. Although there is only a small change of $\tau_{0.01}$ with molecular weight at the lower crystallization temperatures, this dependence becomes very steep at the higher crystallization temperature and is

(31) J. M. G. Fatou and J. M. Banales-Rieuda, *J. Polym. Sci., Part A-2*, 7, 1755 (1969).

(32) L. Mandelkern, J. G. Fatou, and K. Ohno, *ibid., Part B*, 6, 615 (1968).

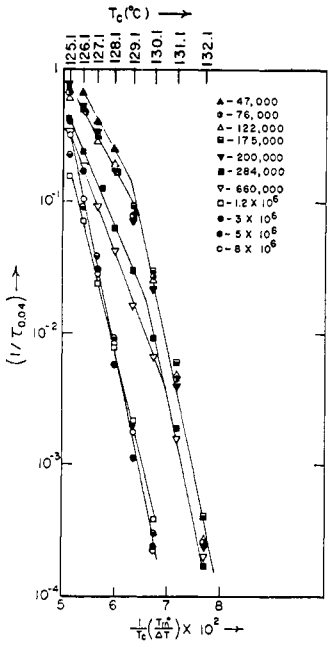

Figure 20. Plot of log $1/\tau_{0.04}$ against $(1/T_c)$ $(T_m^0/\Delta T)$ for indicated molecular weight fractions.

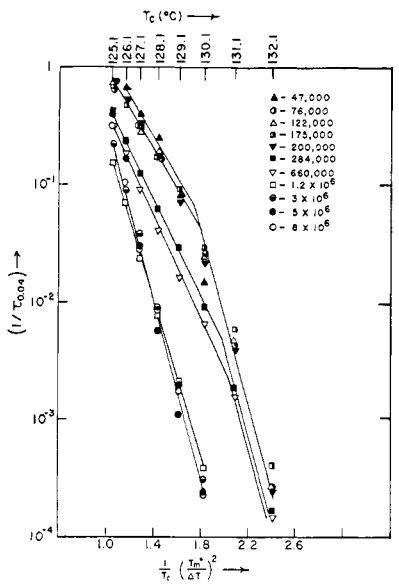

Figure 21. Plot of log $1/\tau_{0.04}$ against $(1/T_c)$ $(T_m^0/\Delta T)$ for indicated molecular weight fractions.

monotonically changing between the extremes. The sharp increase of $\tau_{0.01}$ with chain length precludes, from a practical point of view, studies of very high molecular weight fractions at crystallization temperatures exceeding 130°. We note that the three highest molecular weight fractions, for which the Avrami $n = 2$, have values of $\tau_{0.01}$ which are less than would be anticipated from the samples having slightly lower molecular weights for which $n = 3$. The observation of a maximum in the crystallization rate with molecular weight is not limited to linear polyethylene. Qualitatively similar results have been reported for molecular weight fractions of poly(tetramethyl-*p*-silphenylene siloxane).[33] This phenomenon thus appears to be of general applicability to long-chain molecules.

Temperature Coefficient. The temperature coefficients of the crystallization rate for the individual molecular weight

(33) J. H. Magill, *J. Polym. Sci., Part B*, **6**, 853 (1968).

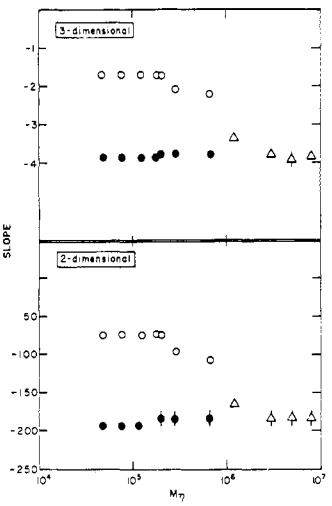

Figure 22. Plot of slopes from straight lines of Figures 20 and 21 against molecular weight: low-temperature lower molecular weights (○), high-temperature lower molecular weights (●), higher molecular weights (△).

fractions were determined from the plots of Figures 20 and 21. These were made in the conventional manner in accord with nucleation theory.[9,30c,34] Consequently, plots are given of log $(1/\tau_{0.04})$ against either of the temperature functions $(1/T_c)(T_m^0/\Delta T)$ or $(1/T_c)(T_m^0/\Delta T)^2$ which represent the extremes of either two or three dimensional nucleation respectively. Here, the time necessary for 4% of the absolute crystallinity to be attained, $\tau_{0.04}$, is taken as the measure of the crystallization rate. T_m^0 was taken as 145.5°. The general character of the plots in Figures 20 and 21 is independent of the nucleation mode chosen, as is well known in other applications.[9,35,36] The purpose here is not to attempt to discriminate between these two possible modes by data of this type. It has been amply demonstrated in the past the temperature coefficient analysis cannot accomplish this task.[9,35,36] In order to avoid complications of the analysis at this point we have not treated the very low molecular weights and have only considered molecular weights where the melting temperature is independent of chain length.

The most striking feature of these figures is that for the molecular weight fractions where the crystallization could be conducted above 130° the plots are nonlinear. For molecular weights 47,000 and for fractions greater than 660,000 a linear relation is obtained in accord with the results that have been reported for a large number of unfractionated polymers.[9] However, in the intermediate molecular weight range, where the higher crystallization temperatures can be attained, the data cannot be given a linear representation. It is now possible to draw two straight lines through the experimental data which intersect usually at the crystallization temperatures of 129–130°. A much smaller slope is obtained from the straight line which represents the data for the lower crystallization temperatures. The fact that this type of behavior can be observed is a consequence of utilizing molecular weight fractions which allow for the attainment of the higher crystallization temperatures.

The slopes of the straight lines from Figures 20 and 21 are plotted as a function of molecular weight in Figure 22. The trends are the same for either of the nucleation modes. For

(34) L. Mandelkern, *J. Appl. Phys.*, **26**, 443 (1955).
(35) L. Mandelkern, N. L. Jain, and H. Kim, *J. Polym. Sci., Part A-2*, **6**, 165 (1968).
(36) C. Devoy, L. Mandelkern, and L. Bourland, *ibid., Part A-2*, **8**, 869 (1970).

Figure 23. Electron micrograph of debris from selective oxidation for $M = 284{,}000$ crystallized at 130.1° for 6 weeks.

Figure 24. Electron micrograph of debris from selective oxidation for $M = 8 \times 10^6$ crystallized at 130.1° for 6 weeks.

molecular weights less than 1.2×10^6, the temperature coefficients for either the high-temperature or low-temperature regions are, within experimental error, independent of chain length. The results for the very high molecular weights appear to indicate a constant value for the slopes, behavior which is very similar to that for the high-temperature range of the lower molecular weights. It becomes quite clear from this extensive set of data now available that although the very strong negative temperature coefficients still give strong support to the importance of nucleation processes, they are not as simple as has been heretofore postulated.[9]

Crystallite Morphology. Since there is a strong influence of molecular weight on all aspects of the crystallization process, it is pertinent to ascertain whether there are any concomitant changes in the primary morphological forms that develop. We focus attention here on the crystallite structure. From studies of replicas of fracture surfaces of unfractionated polymers[37,38] and of molecular weight fractions of linear polyethylene, up to and including $M = 5 \times 10^5$,[5] it has been established that a lamella-like crystallite is the primary morphological structure of bulk-crystallized samples. For higher molecular weight fractions, which are of particular interest in the present context, the debris remaining after selective oxidation has been examined by electron microscopy. Some typical results from this study are shown in Figures 23 and 24, which represent samples of $M = 2.84 \times 10^5$ and $M = 8 \times 10^6$, respectively, which were crystallized at 130.1° for long time periods. In both examples, lamella-like crystallites are observed. For molecular weights equal to or less than 2.84×10^5, they are well defined and quite large in their lateral dimensions. For the higher molecular weights, although the lamella are still easily discerned, they are not as well defined and their lateral dimensions are smaller. Thus we find that lamella-like crystallites are formed over the complete molecular weight range studied. Therefore, the differences in the crystallization kinetics and the associated changes in properties, with molecular weight, cannot be attributed to any major differences in the basic crystallite morphology.

Conclusion and Summary

We have in the foregoing attempted to synthesize a large amount of new experimental data concerned with the influence of molecular weight on crystallization from the melt. Certain major features have emerged from this study which hopefully will serve as the basis for developing a coherent theoretical and molecular understanding of the crystallization process. At this point, we do not attempt such an undertaking, but summarize some of the important factors which have not been apparent from the many similar experimental studies that have been conducted on unfractionated polymers.[9]

Although deviations from the Avrami formulation of the kinetics of phase change are well known for long-chain molecules, it is now found that the onset of these deviations is very systematic with molecular weight and crystallization temperature. The extent of the transformation at which departures from theory are first discerned correlates with the final level of crystallinity that is attained. This latter factor in turn governs the properties of the crystalline polymers. It has been found that when the data are analyzed in detail there is surprisingly little difference with respect to the fit of experimental data between the Göler–Sachs free-growth and Avrami theories. For the early stages of the transformation, which adheres to these most simple theories, the Avrami exponent n is found to be an integer which depends on molecular weight. For the lowest molecular weights, this quantity is found to be four and is reduced to two at the very highest molecular weights. For very high temperatures of crystallization, much closer adherance to the theory is observed.

Besides the isotherm shape and final level of crystallinity that is attained, the crystallization rate, at a fixed temperature, is also markedly dependent on the chain length. A maximum is found in the crystallization rate. The molecular weight at the maximum is dependent on the crystallization temperature. The utilization of molecular weight fractions has enabled isothermal crystallization to be studied at higher temperatures than have been heretofore attainable. One consequence of the additional data that have been obtained is the observation that the temperature coefficient of crystallization does not adhere to the formal aspects of simple nucleation theory as has been supposed.

The kinetic data that have been reported here make it abundantly clear that the properties of crystalline polymers are a consequence of kinetic factors. It is hoped that sufficient basic data are now provided by which to proceed from a phenomenological description to a molecular understanding of the crystallization process.

(37) F. R. Anderson, *J. Polym. Sci., Part C*, No. 3, 123 (1963).
(38) F. R. Anderson, *J. Appl. Phys.*, 35, 64 (1964).